ACS OMEGA

http://pubs.acs.org/journal/acsodf

Article

Antiviral Activity against SARS-CoV-2 of Conformationally Constrained Helical Peptides Derived from Angiotensin-Converting Enzyme 2

Michael Quagliata, Maria Alfreda Stincarelli, Anna Maria Papini, Simone Giannecchini, and Paolo Rovero*

Cite This: *ACS Omega* 2023, 8, 22665−22672

Read Online

ACCESS | Metrics & More | Article Recommendations | Supporting Information

ABSTRACT: Despite the availability of vaccines, COVID-19 continues to be aggressive, especially in immunocompromised individuals. Therefore, the development of a specific therapeutic agent with antiviral activity against SARS-CoV-2 is necessary. The infection pathway starts when the *receptor binding domain* of the viral spike protein interacts with the *angiotensin converting enzyme 2* (ACE2), which acts as a host receptor for the RBD expressed on the host cell surface. In this scenario, ACE2 analogs binding to the RBD and preventing the cell entry can be promising antiviral agents. Most of the ACE2 residues involved in the interaction belong to the α1 helix, more specifically to the minimal fragment ACE2(24−42). In order to increase the stability of the secondary structure and thus antiviral activity, we designed different triazole-stapled analogs, changing the position and the number of bridges. The peptide called **P3**, which has the triazole-containing bridge in the positions 36−40, showed promising antiviral activity at micromolar concentrations assessed by plaque reduction assay. On the other hand, the double-stapled peptide **P4** lost the activity, showing that excessive rigidity disfavors the interaction with the RBD.

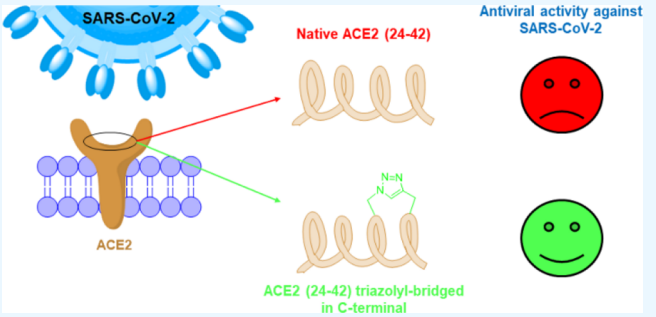

INTRODUCTION

In December 2019, the first case of severe acute respiratory syndrome coronavirus 2 (SARS-CoV-2) infection was diagnosed in the city of Wuhan. Since then, the virus infected over 649 million people and caused over 6.6 million deaths worldwide.[1] The disease related to SARS-CoV-2 infection, termed coronavirus disease 19 (COVID-19), can be a mild asymptomatic illness or cause a wide range of symptoms, ranging from a simple cold to severe, even fatal pneumonia. The development of efficient vaccines represented a real milestone in the prevention of this disease, which, however, still remains aggressive in immunocompromised subjects.[2,3] Complementary to vaccination, it is therefore important to develop antiviral drugs against SARS-CoV-2. Two antiviral drugs are currently available to treat infected individuals with a high risk of developing severe disease. Molnupiravir (Lagevrio) exerts its antiviral action by introducing copy errors during viral RNA replication.[4−6] On the other hand, Nirmatrelvir (Paxlovid) acts as an orally active SARS-CoV-2 protease inhibitor.[7−9] However, other therapeutic agents are necessary, not only to diversify the mechanism of action but also to make the therapy more specific. In this scenario, the specific molecular mechanisms by which the virus recognizes and infects the target cells, that is, the entry process, appear as an appealing target for the development of specific therapeutic agents, potentially able to block the virus before the infection. This approach has been successfully implemented in the case of several different viruses, including human immunodeficiency virus (HIV) and Ebola virus (EboV).[10,11]

The mechanism of SARS-CoV-2 entry into cells is complex, being based on three molecular events that can be targeted to block cell infection,[12] whose key player is the viral spike glycoprotein, located on the surface of the viral membrane envelop. The spike glycoprotein of SARS-CoV-2 is a trimeric protein, which exists in metastable prefusion conformation that undergoes a substantial structural rearrangement during the interaction with the host cell and is composed of the subunits S1 and S2.[13] Initially, the *receptor binding domain* (RBD) of the spike glycoprotein recognizes the *angiotensin converting enzyme 2* (ACE2) expressed on the host cell surface.[14] This interaction produces a conformational change in the spike glycoprotein that enables the proteolytic cleavage of its S1 subunit by the

Received: March 3, 2023
Accepted: May 16, 2023
Published: June 13, 2023

https://doi.org/10.1021/acsomega.3c01436
ACS Omega 2023, 8, 22665−22672

transmembrane protease serine 2 (TMPRSS2) of the host cell. Subsequently, subunit S2 changes the conformation by inserting the *fusion peptide* (FP) into the cell membrane and triggering the association between the *heptad repeat 1* and *heptad repeat 2* (HR1 and HR2) domains to form a six helix bundle (6-HB), which brings the viral and cellular membranes in close proximity for fusion.[15,16]

The complex entry mechanism described above suggests several interesting molecular targets for the development of new antiviral agents. Indeed, several studies were focused on the very first event, the binding of RBD to ACE2, aiming at the development of inhibitors of this protein−protein interaction. Two complementary strategies can be envisaged: the first one aims at the development of ACE2 inhibitors, that is, molecules capable of occupying the binding site on ACE2, while the second one focuses on RBD binders, able to compete with ACE2. Villa et al. synthesized aptamers binding to the region surrounding the K353 in ACE2, which is reported as a key residue for interaction.[17] However, it should be noted that the antiviral use of ACE2 inhibitors is afflicted with a relevant drawback, that is the potential to inhibit the physiological function(s) of a key enzyme such as ACE2. Accordingly, molecules capable of binding to the RBD appear much more promising, and the binding site of ACE2 is indeed an interesting template for the rational design of such molecules. The cryo-EM structure of the ACE2-spike S1 complex (PDB: 6M0J) shows that most of the ACE2 residues involved in the protein−protein interaction (PPI) belong to helix α1, corresponding to the sequence ACE2(23−52).[18,19] In particular, the key residues are Asn,[24] Thr,[27] Asp,[30] Lys,[31] His,[34] Glu,[35] Glu,[37] Asp,[38] Tyr,[41] and Gln.[42] Some publications report α1 fragments capable of interacting with the RBD.[20,21] Nevertheless, linear peptides derived from the α1 sequence do not maintain a helical structure in solution and thereby display limited ability to efficiently bind to the RBD.[22,23] In light of these considerations, many reported potential inhibitors of ACE2-RBD interaction are based on this N-terminal domain of ACE2 modified to increase the conformational propensity to form an a-helix.

In this perspective, a series of ACE2(23−52)-derived antiviral peptides were designed by substituting residues not involved in the PPI with residues that will contribute to a-helix stability. For example, the hACE2(19−45)-derived peptide P10 designed by Karoyan et al. is characterized by a high content of leucine residues, aiming to increase the helical content, together with the substitution of Ala[25] with an L-homotyrosine (*h*Tyr) residue.[24] This modified sequence showed a promising higher binding affinity (K_d = 0.03 nM) assessed by biolayer interferometry.[25] Likewise, Odolczyk et al. synthesized a modified hACE2(30−35)-derived hexapeptide with Phe[32] replacing the Gly residue, which is capable of binding to the RBD fragment (K_d = 210 ± 50 nM) in a microscale thermophoresis experiment.[26] In a recent publication, Schmalz et al. reported N-capped peptides with the rigidified diproline-derived module termed *βHAsp*-ProM-5, to increase the α helical content.[27] Despite a significant increase in secondary structure stability, the binding affinity of the peptide remains modest (K_d = 1.21 ± 0.36 μM) in microscale thermophoresis (MST). On the other hand, N-capping with the non-natural motif *βHAsp-Pro-Pro* enhances the affinity (K_d = 0.062 ± 0.017 μM) without increasing the helical content.[28] Stabilization of the secondary structure is frequently obtained by side chain-to-side chain cyclization, leading to macrocycles often called "stapled peptides", referring to any short sequence, that has the propensity for α-helical conformation that is constrained by a variety of cross-link synthetic strategies.[29] The simplest one is side chain-to-side chain lactam bridge formation.[30] Maas et al. exploited this reaction to obtain different ACE2(21−55) stapled analogs. The sequence bridged at the position $i-i$ + 4, that is, 36−40 is able to inhibit the Spike-ACE2 PPI (IC_{50} = 3.6 μM).[31] Another widely used method is the alkenyl bridge formation by ring closing metathesis (RCM)[32] exploited by Curreli et al. who designed four double-stapled peptides displaying antiviral activity (IC_{50} of 1.9 to 4.1 μM). Moreover, one of the fragment was able to bind the RBD with a K_d = 2.2 μM, as determined by surface plasmon resonance (SPR) experiments.[33] Similarly, a stapled analog of ACE2(34−42) was capable of inhibiting the RBD-ACE2 interaction (IC_{50} = 21.7 ± 7 μM) in ELISA.[34]

As mentioned above, most of the ACE2 residues involved in the RBD-ACE2 PPI belong to the helix α1. In addition, there are four residues spatially close to α1, namely L353, G354, D355, and R357, which are located on the β sheets β3 and β4, interacting with the RBD. In this scenario, the heptapeptide GK-7, corresponding to the sequence ACE2(352−358), was reported to exhibit an interesting dissociation constant (K_d = 25.1 nM) measured in Biolayer interferometry and also displayed a moderate antiviral activity in vitro (IC_{50} = 2.96 μg/mL).[35] To improve binding affinity, other authors reported different chimeric stapled helical peptides composed of the two key fragments in ACE2. For example, Sarto et al. designed a conformational stapled chimera called p6cyc with a K_d = 270 ± 140 nm, assessed by microscale thermophoresis (MST) using the RBD. Similarly, Shah et al. synthesized a double stapled peptide bearing a lactam bridge in the α1 portion and a disulfide bridge in the β4 one that showed a promising antiviral activity in vitro (IC_{50} = 0.37 μM).[36] In addition to peptides, miniproteins were reported to bind to the RBD. One of these miniproteins, termed LCB1, folds into three distinct α-helices and has a potent antiviral activity in vitro (IC_{50} = 23.54 pM).[37] Given the length of LCB1 (55 residues), Weißenborn et al. synthesized a cyclic truncated analog of LCB1, called LW25.13, which also maintained a strong antiviral activity (IC_{50} = 630 ± 240 pM).[38] Finally, there are several antiviral peptides studied *in silico* as potential inhibitors of ACE2-RBD PPI. For example, Panda et al. designed a potential inhibitor based on α1, making single-point mutations on non-key residues. The most promising peptide is the one that simultaneously contains all the individual mutations (IDWQFWFHYDKWDHEWEDEWYQSS).[39] Similarly, Basit et al. proposed an α1-based sequence (EAAAKAKLS-NENHDNSTVSF), which has a lower predicted binding affinity for the RBD (−13.2 kcal/mol) than the native sequence (−10.2 kcal/mol).[40] It should be noted that the large majority of the multitude of studies reporting putative anti-SARS-CoV-2 peptides are based on binding affinity measurements, performed with different available techniques, while very few report the real antiviral activity, measured in cell systems. The lack of this information hampers the possibility to evaluate the real potential of these products as candidate antiviral agents.

With all these considerations in mind, we designed and synthesized a series of α1-ACE2 stapled analogs based on the minimal fragment ACE2(24−42). In order to stabilize the secondary structure, we introduced one or two *i*-to-*i* + 4 side chain-to-side chain triazole bridge formation by copper(I)-

https://doi.org/10.1021/acsomega.3c01436
ACS Omega 2023, 8, 22665−22672

Table 1. Peptide Sequences

Peptide	Linear precursor	1,4-[1,2,3]triazolyl containing cyclo-peptides
ACE2(24-42)	QAKTFLDKFNHEAEDLFYQ	-
P1 [Nle(ε-N_3)^{28} (&^{1}), Pra^{32} (&^{2})]ACE2(24-42)	QAKT-Nle(ε-N_3)-LDK-Pra-NHEAEDLFYQ	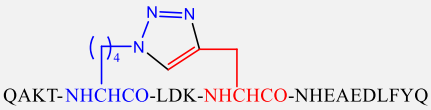 QAKT-NHCHCO-LDK-NHCHCO-NHEAEDLFYQ
P2 [Nle(ε-N_3)^{32} (&^{1}), Pra^{36} (&^{2})]ACE2(24-42)	QAKTFLDK-Nle(ε-N_3)-NHE-Pra-EDLFYQ	 QAKTFLDK-NHCHCO-NHE-NHCHCO-EDLFYQ
P3 [Nle(ε-N_3)^{36} (&^{1}), Pra^{40} (&^{2})]ACE2(24-42)	QAKTFLDKFNHE-Nle(ε-N_3)-EDL-Pra-YQ	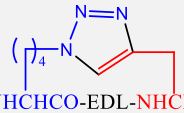 QAKTFLDKFNHE-NHCHCO-EDL-NHCHCO-YQ
P4 [Pra^{28} (&^{1}), Nle(ε-N_3)^{32} (&^{2}); Nle(ε-N_3)^{36} (&^{1}), Pra^{40} (&^{2})]ACE2(24-42)	QAKT-Pra-LDK-Nle(ε-N_3)-NHE-Nle(ε-N_3)-EDL-Pra-YQ	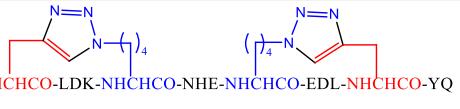 QAKT-NHCHCO-LDK-NHCHCO-NHE-NHCHCO-EDL-NHCHCO-YQ

[a] Nle(ε-N_3): L-ε-azido norleucine; Pra: L-propargylglycine.

catalyzed azide−alkyne cycloaddition (CuAAC),[41] an approach that, to the best of our knowledge, has not been systematically explored in the design of ACE2-derived analogs as SARS-CoV-2 antiviral candidates. The conformational preferences of the peptides were analyzed by circular dichroism(CD), and the antiviral activity against SARS-CoV-2 was tested in vitro by plaque reduction assays (PRAs). The results obtained provide a structure−activity correlation study that can serve as a sound foundation for the development of new ACE2 analogs endowed with antiviral activity.

RESULTS AND DISCUSSION

Peptide Analog Design and Synthesis. In light of the considerations mentioned above, we selected the ACE2 minimal fragment containing all the amino acid residues involved in the interaction with the SARS-CoV-2 spike glycoprotein RBD, that is, ACE2(24−42). With the aim to stabilize the α-helical structure of this peptide, we stapled its sequence placing one or two triazole bridges in different positions, according to the click-chemistry approach based on copper(I)-catalyzed azide−alkyne cycloaddition (CuAAC), introduced into peptides by the recently recognized Nobel prize winner, Morten Meldal, to produce conformationally constrained analogs of many bioactive peptides, including ours.[41,42] In fact, the triazolyl moiety, isostere of the amide bond, can be easily formed in biorthogonal conditions, without affecting unprotected amino acid side chains, thus obtaining a conformational constraint that may enhance target specificity and/or biological potency, as compared to the linear, unmodified peptides.[43−45] Generally speaking, drug-like properties of the new compounds are improved since the stapling triazolyl enhances its in vivo resistance to enzymatic degradation.[46,47] Initially, we have introduced in the ACE2(24−42) sequence, a single side chain-to-side chain i to i + 4 triazolyl-containing bridge-modifying positions located in the center of the sequence that are not directly involved in RBD binding, that is, 28−32, 32−36, and 36−40. In order to obtain the singularly modified triazolyl-containing analogs, we introduced two different non-natural residues, namely, L-ε-azido norleucine (Nle(ε-N_3)) and L-propargylglycine (Pra) in the i and i + 4 positions, restrictively. The triazolyl moiety is flanked by a total of 5 methylenes, 4 on the N-terminal proximal- and 1 on the C-terminal proximal side, flanking the 1,4-triazolyl moiety, which has been previously reported to be the optimal length to stabilize the α-helical structure.[48] Accordingly, as shown in Table 1, the conformational constraint in position 28−32 was obtained replacing Phe^{28} by Nle(ε-N_3) and Phe^{32} by Pra, obtaining, after CuAAC reaction, the stapled cyclopeptide **P1**, with the triazole bridge in 1,4 orientation. Similarly, we obtained peptides **P2** and **P3**, bearing the triazole bridge in the positions 32−36 and 36−40, respectively. Finally, we designed and synthesized peptide **P4**, containing a double staple, involving positions 28−32 and 36−40. In this case, the bridge connecting positions 28−32 was obtained in the 4,1 orientation and 5 methylenes in 1 + 4 permutation, while the second one, 36−40, was constructed in the opposite orientation (1,4) and with the 5 methylenes in 4 + 1 permutation. This strategy was designed in order to avoid a possible unwanted cyclization between positions 32 and 36. This topology of the triazole bridges was anticipated to support the conformational propensity of this sequence in the native a1 helix conformation since it was reported that there is no negative effect on the stabilization of the helix by reversing the triazolyl orientation.[47,48] The linear precursors were prepared by microwave-assisted solid-phase peptide synthesis (MW-SPPS), following the 9-fluorenylmethoxycarbonyl (Fmoc)/tBu orthogonal protection strategy. Cyclization was performed on resin, using CuBr, 2,6-lutidine, and DIPEA under microwave irradiation, employing a procedure recently optimized in our laboratory.[49] All the peptides were purified to homogeneity by flash reverse-phase liquid chromatography (RP-LC) and analytically characterized by analytical HPLC coupled to a

https://doi.org/10.1021/acsomega.3c01436
ACS Omega 2023, 8, 22665−22672

single quadrupole ESI-MS. Full analytical data (Rt, purity, and MS characterization) are reported in Table S1.

Circular Dichroism. The secondary structure propensity of the stapled analogs was studied by circular dichroism(CD) spectroscopy performed both in H_2O and in the H_2O:TFE 1:1 (v/v) mixture at 200 μM concentration (Figure 1), in

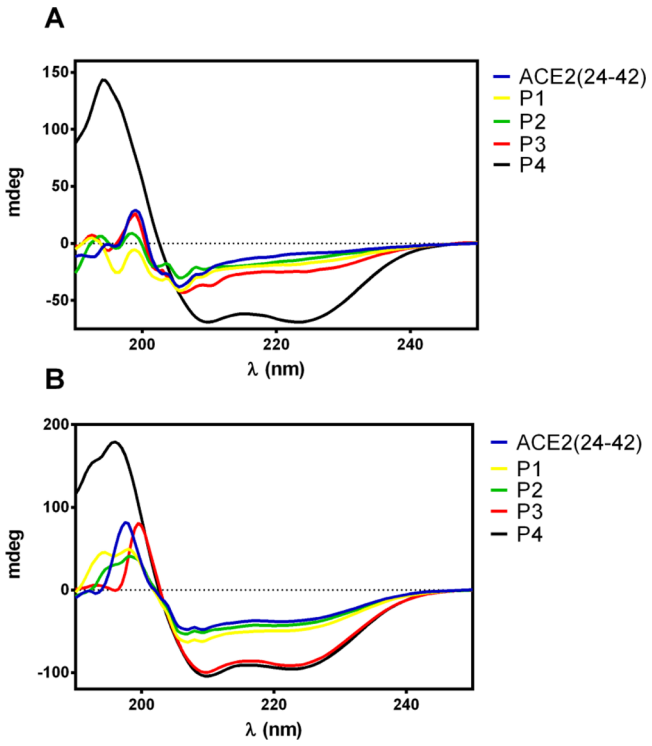

Figure 1. Comparative analysis of CD spectra of ACE2(24−42) and **P1**−**P4** peptides in (A) H_2O and (B) H_2O:TFE 1:1.

comparison with the linear native peptide sequence ACE2(24−42). These solutions appeared stable over time, indicating that no aggregation occurred. Already in water, **P3** (containing one single triazolyl bridge in 36−40), and **P4** (containing a second triazolyl bridge in 28−32) showed a high tendency to assume an α-helical secondary structure. On the other hand the other stapled analogs **P1** and **P2** and the parent peptide (ACE2(24−42) showed a random coil conformation (Figure 1). As expected, in the H_2O:TFE (1:1) mixture, the effect of TFE induces in all the peptides a more ordered structure.[50]

Interestingly, simulation by the online tool BestSel confirmed the experimental CD analysis, suggesting that in H_2O:TFE (1:1) the stapled peptides **P1** and **P2** (triazolyl-containing bridge in 28−32 and 32−36, respectively) have a lower tendency to form an α-helical structure than the linear peptide ACE2(24−42) compared to **P3** (triazolyl-containing bridge in 36−40) that has an α-helix propensity similar to that of the linear reference peptide. On the other hand, **P4** (with two triazolyl-containing bridges) is strongly structured and almost completely folded as an α-helix (Table 2).

Antiviral Activity and Cytotoxicity. The antiviral activity of all the stapled peptide analogs of the linear native peptide ACE2(24−42) was evaluated against SARS-CoV-2 in Vero E6 cells using the inhibitory viral plaque reduction assay (PRA). All the clicked peptides, except **P2**, feature improved antiviral activity, compared to ACE2(24−42). In particular, **P3** ([Nle(ε-N_3)[36] (&[1]), Pra[40] (&[2])]ACE2(24−42)) containing one single side chain-to-side chain triazolyl bridge in 36−40 shows a significant dose-dependent antiviral activity at micromolar concentrations (Figure 2). Cell cytotoxicity was tested by the MTT reduction assay in Vero E6 cells, indicating that none of the tested peptides exerted significant toxicity (Figure S2).

According to the CD spectra, all the peptides showed a tendency to assume a α-helical secondary structure in structuring the solvent like the H_2O:TFE 1:1 (v/v) mixture.[50,51] Differently, only the analogs **P3** and **P4** maintain a tendency to form an α-helix in water. Significant antiviral activity against SARS-CoV-2 (evaluated by PRA) was significant. The lack of antiviral activity of the native ACE2(24−42) indicates that stabilization of the secondary structure, by stapling positions 36−40 is fundamental to reproduce the correct side chain orientation required for optimal interaction of the ACE2 derived peptide with the RBD domain in the Spike protein. This helix stabilizing effect increases by shifting the position of the staple toward the C-terminal part of the sequence or by introducing a second staple, which is located at position 18−32, that by itself did not contribute to increase in helicity relative to the parent peptide (cf. **P1** and **ACE2(24−42)**). However, the very high conformational stabilization of **P4** is associated with excessive rigidity and appears to compromise its antiviral activity. In fact, significant antiviral activity (evaluated by PRA) is observed only in the mono-stapled but more flexible analog **P3** in which the triazolyl-containing bridge is located upstream, as compared to **P1** and **P2**, conferring a conformational propensity quite similar to that observed with the parent native ACE2 fragment.

In conclusion, we report herein that the triazole stapling of a short peptide derived from the α1-ACE2 helix can stabilize its helical conformation, yielding an analog with enhanced antiviral activity against SARS-CoV-2 relative to the native parent peptide. Up to now, similar results were obtained only with much longer peptide sequences (about 40 residues)[38] and complex sequence modifications requiring more demanding syntheses,[33,36] or short peptides that are easily degradable in vivo and therefore have a lower drug-like propensity.[35] Accordingly, the triazolyl bridged peptide **P3** represents an

Table 2. Simulation of Percentage of the Secondary Structure of CD in H_2O:TFE (1:1) and in H_2O (in Bracket) Evaluated Using the Online Tool BestSel

peptide	α-helix	β-strand	β-turn	random coil
ACE2(24−42)	63.3 (8.8)	23.6 (15.1)	13.1 (14.7)	0.0 (61.3)
P1	40.1 (5.4)	13.5 (22.9)	8.5 (16.9)	37.9 (54.7)
P2	37.3 (7.7)	15.7 (25.8)	10.2 (14.6)	36.8 (51.9)
P3	57.0 (34.6)	32.8 (31.7)	5.2 (25.1)	5.0 (8.6)
P4	96.2 (49.5)	0.0 (1.5)	3.8 (7.0)	0.0 (42.0)

https://doi.org/10.1021/acsomega.3c01436
ACS Omega 2023, 8, 22665−22672

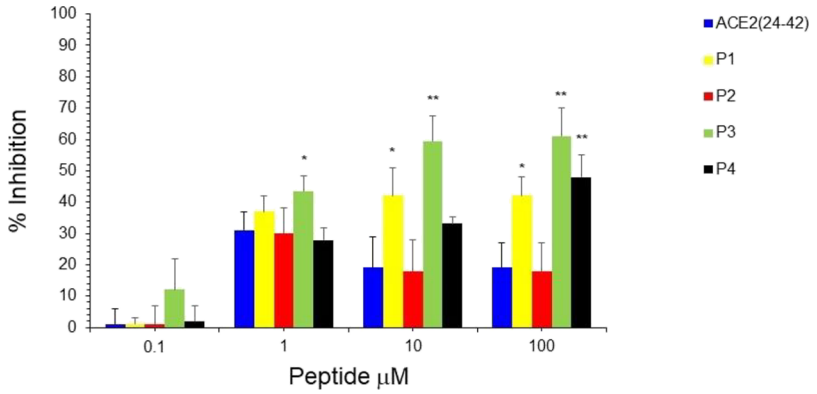

Figure 2. Antiviral activity of ACE2(24−42) and clicked peptides **P1−P4** against SARS-CoV-2 in Vero E6 cells. SARS-CoV-2 infection of Vero E6 cells at MOI of 0.01 in the presence of all the peptides at indicated concentration was assayed with the viral plaque reduction assay. Data represent means ± standard deviation. Asterisk shows that the inhibitory activity of the peptide was significantly different from that of the linear native peptide ACE2(24−42) at $p < 0.05$ * and $P < 0.01$ ** (*Student's t-test*).

interesting lead for the development of anti-SARS-CoV-2 peptidomimetics with enhanced metabolic stability and synthesized through an advantageous bioorthogonal methodology.

EXPERIMENTAL SECTION

Reagents. All Fmoc-protected amino acids, *N*,*N*′-diisopropylcarbodiimide (DIC) and oxyma (ethyl cyanohydroxyiminoacetate), were purchased from Iris Biotech GmbH (Marktredwitz, Germany). Dichloromethane (DCM), piperidine, triisopropylsilane (TIS), and trifluoroacetic acid (TFA) were purchased from Sigma-Aldrich (Milano, Italy). Tentagel S RAM resin was purchased from Rapp Polymere (Tuebingen, Germany). Acetonitrile and peptide synthesis-grade *N*,*N*-dimethylformamide were purchased from Carlo Erba (Milano, Italy).

MW-Assisted Solid-Phase Peptide Synthesis. The peptides were synthesized using the Liberty Blue automated microwave peptide synthesizer (CEM Corporation, Matthews, NC, USA) following the Fmoc/*t*Bu strategy and using Tentagel S RAM resin (loading 0.23 mmol/g) as previously described.[52] The following Fmoc-amino acids were used: Fmoc-Ala-OH, Fmoc-Asp(tBu)-OH, Fmoc-Glu(tBu)-OH, Fmoc-Phe-OH, Fmoc-His(Trt)-OH, Fmoc-Lys(Boc)-OH, Fmoc-Leu-OH, Fmoc-Asn(Trt)-OH, Fmoc-Gln(Trt), Fmoc-Thr(tBu)-OH, Fmoc-Tyr(tBu)-OH, Fmoc- Nle(ε-N_3)-OH, and Fmoc-Pra-OH. The Fmoc deprotections were performed using a solution of 20% piperidine in DMF (2 M). The coupling steps were performed using Fmoc-protected amino acids (5 equiv, 0.4 M) and a mixture of DIC (5 equiv, 0.5 M) and OxymaPure (5 equiv, 1 M). Finally, N-acetylation was performed using Ac_2O (10% v:v in DMF) for 10 min. The cleavage and side-chain deprotections were performed using a cocktail cleavage composed by TFA/TIS/H_2O (95:2.5:2.5, v:v:v) at room temperature for 2.5 h. Then, the resin was filtered, followed by precipitation with cold Et_2O. The suspensions were centrifuged and lyophilized. The crude peptides were purified by reverse-phase flash liquid chromatography (RP-LC) using a SNAP ultra C18 column 12 g at 12 mL/min as solvent systems A (0.1% TFA in H_2O) and B (0.1% TFA in ACN). The purified peptides were characterized by RP-HPLC-MS using a Waters ACQUITY HPLC equipped with a Waters ZQ Detector, supplied with a BEH C18 1.7 μm, 2.1 × 50 mm column at 0.6 mL/min using solvent systems A and B previously described. All the characterization data are reported in the Supplementary Material (Figures S1−S5). Click reaction was performed on resin as previously described.[49]

Circular Dichroism. CD spectra of the peptides were recorded using a JASCO J-810 CD spectropolarimeter at 25 °C. The spectrum was measured using a quartz cells of 0.1 cm path length in the 260−190 nm spectral range, 4 accumulations, 50 nm/min scanning speed, and 1 nm bandwidth. The peptides were dissolved in H_2O or H_2O:TFE 1:1 (v/v) at a concentration of 200 μM. The secondary structure content was predicted using the online BestSel.[53]

Antiviral Activity. Antiviral activity against SARS-CoV-2 was tested on Vero E6 cells using the inhibitory viral plaque reduction assay (PRA). The cell propagation medium was performed in Dulbecco's modified eagle's medium (DMEM) supplemented with 10% fetal bovine serum (FBS) and with 1% penicillin/streptomycin. SARS-CoV-2 stock, consisting of cell-free supernatants of acutely infected Vero E6 cells, was aliquoted and stored at −80 °C until use. Titration of the viral stocks expressed as plaque forming unit (PFU) was carried out in Vero E6 cells. SARS-CoV-2 was used to infect Vero E6 cell lines in duplicate, and viral plaques were visualized 3 days after infection. Briefly, 6-well plates were seeded with 2.5×10^5 cells in 3 mL of growth medium and kept overnight at 37 °C with 5% CO_2. In order to produce a 0.01 multiplicity of infection (MOI), before the infection, the SARS-CoV-2 viral stock was mixed 1:1 in a final volume of 0.3 mL with 10-fold serial dilutions (final concentrations of 100, 10, 1, and 0.1 μM) of all the synthetic peptides ACE2(24−42) and **P1-P4** (in DMSO) used as inhibitors and immediately added onto the cell substrate and incubated for 1 h at 37 °C with 5% CO_2. The SARS-CoV-2 treated with DMSO was used as the control. Then, the cells were washed with PBS, and the overlay medium composed of 0.5% sea plaque agarose diluted in propagation medium, was added to each well. After 3 days incubation at 37 °C, the monolayers were fixed with methanol and stained with 0.1% crystal violet and the viral titers were calculated by PFU counting. Percentage of plaque reduction activity was calculated by dividing the average of PFU obtained in the presence of the different peptide samples by the average of PFU obtained in the presence of DMSO (viral positive

https://doi.org/10.1021/acsomega.3c01436
ACS Omega 2023, 8, 22665−22672

control). All experimental procedures were conducted under biosafety level 3 (BSL3) containment.

Cell Cytotoxicity Assay. The cytotoxicity was evaluated by MTT reduction assay. Vero E6 cells were plated at a density of 10^4 cells per well in a flat-bottom 96-well culture plate and allowed to adhere overnight. When the cell layers were confluent, the medium was removed, the wells were washed twice with PBS, and treated with 100 μL of MEM in DMSO or with the appropriate concentrations of the different synthetic peptides developed in this study. The final solutions of the peptide (0.1−100 μM) were added to the cells and incubated at 37 °C in a CO_2 incubator for 72 h. After treatment, an MTT kit (Roche, Milano, Italy) was used according to the supplier's instructions, and the absorbance of each well was measured using a microplate spectrophotometer at λ = 595 nm. Cytotoxicity was calculated by dividing the average optical density of the treated samples by the average of the mock-treated samples in the presence of DMSO.

■ ASSOCIATED CONTENT

Supporting Information

The Supporting Information is available free of charge at https://pubs.acs.org/doi/10.1021/acsomega.3c01436.

Full analytical data of the peptides and cell cytotoxicity assay (PDF)

■ AUTHOR INFORMATION

Corresponding Author

Paolo Rovero − *Interdepartmental Research Unit of Peptide and Protein Chemistry and Biology, Department of NeuroFarBa, University of Florence, 50019 Sesto Fiorentino, Italy;* orcid.org/0000-0001-9577-5228; Email: paolo.rovero@unifi.it

Authors

Michael Quagliata − *Interdepartmental Research Unit of Peptide and Protein Chemistry and Biology, Department of Chemistry "Ugo Schiff", University of Florence, 50019 Sesto Fiorentino, Italy;* orcid.org/0000-0003-0891-3405

Maria Alfreda Stincarelli − *Department of Experimental and Clinical Medicine, University of Florence, 50134 Florence, Italy*

Anna Maria Papini − *Interdepartmental Research Unit of Peptide and Protein Chemistry and Biology, Department of Chemistry "Ugo Schiff", University of Florence, 50019 Sesto Fiorentino, Italy;* orcid.org/0000-0002-2947-7107

Simone Giannecchini − *Department of Experimental and Clinical Medicine, University of Florence, 50134 Florence, Italy*

Complete contact information is available at: https://pubs.acs.org/10.1021/acsomega.3c01436

Notes

The authors declare no competing financial interest.

■ ACKNOWLEDGMENTS

The PhD scholarship of MQ is funded by the "Progetto Ministeriale Dipartimenti di Eccellenza 2018-2022" (58503_DIPECC-C.U.P. B96C17000200008).

■ ABBREVIATIONS

ACN, acetonitrile; Boc, t-butyloxycarbonyl; CD, circular dichroism; COVID-19, coronavirus disease 19; CuBr, copper bromide; DMSO, dimethylsulfoxide; DIPEA, *N,N*-diisopropylethylamine; IC_{50}, half maximal inhibitory concentration; ESI-MS, Electrospray Ionization-Mass Spectrometry; Et_2O, diethyl ether; Fmoc, fluorenylmethyloxycarbonyl; MEM, 2-methoxyethoxymethyl; MTT, 3-(4,5-dimethylthiazol-2-yl)-2,5-diphenyltetrazolium bromide; PBS, phosphate-buffered saline; SARS-CoV-2, severe acute respiratory syndrome coronavirus 1; SPPS, solid-phase peptide synthesis; tBu, tert-Butyl; TFE, 2,2,2-trifluoroethanol; Trt, trityl

■ REFERENCES

(1) World Health Organization. Weekly epidemiological update on COVID-19 - 21 December 2022 https://www.who.int/publications/m/item/covid-19-weekly-epidemiological-update---21-december-2022 (accessed Dec 26, 2022).

(2) Lee, A. R. Y. B.; Wong, S. Y.; Chai, L. Y. A.; Lee, S. C.; Lee, M. X.; Muthiah, M. D.; Tay, S. H.; Teo, C. B.; Tan, B. K. J.; Chan, Y. H.; Sundar, R.; Soon, Y. Y. Efficacy of Covid-19 Vaccines in Immunocompromised Patients: Systematic Review and Meta-Analysis. *BMJ* **2022**, *376*, No. e068632.

(3) Duly, K.; Farraye, F. A.; Bhat, S. COVID-19 Vaccine Use in Immunocompromised Patients: A Commentary on Evidence and Recommendations. *Am. J. Health Syst. Pharm.* **2022**, *79*, 63−71.

(4) Toots, M.; Yoon, J.-J.; Hart, M.; Natchus, M. G.; Painter, G. R.; Plemper, R. K. Quantitative Efficacy Paradigms of the Influenza Clinical Drug Candidate EIDD-2801 in the Ferret Model. *Transl. Res.* **2020**, *218*, 16−28.

(5) Kabinger, F.; Stiller, C.; Schmitzová, J.; Dienemann, C.; Kokic, G.; Hillen, H. S.; Höbartner, C.; Cramer, P. Mechanism of Molnupiravir-Induced SARS-CoV-2 Mutagenesis. *Nat. Struct. Mol. Biol.* **2021**, *28*, 740−746.

(6) Malone, B.; Campbell, E. A. Molnupiravir: Coding for Catastrophe. *Nat. Struct. Mol. Biol.* **2021**, *28*, 706−708.

(7) Owen, D. R.; Allerton, C. M. N.; Anderson, A. S.; Aschenbrenner, L.; Avery, M.; Berritt, S.; Boras, B.; Cardin, R. D.; Carlo, A.; Coffman, K. J.; Dantonio, A.; Di, L.; Eng, H.; Ferre, R.; Gajiwala, K. S.; Gibson, S. A.; Greasley, S. E.; Hurst, B. L.; Kadar, E. P.; Kalgutkar, A. S.; Lee, J. C.; Lee, J.; Liu, W.; Mason, S. W.; Noell, S.; Novak, J. J.; Obach, R. S.; Ogilvie, K.; Patel, N. C.; Pettersson, M.; Rai, D. K.; Reese, M. R.; Sammons, M. F.; Sathish, J. G.; Singh, R. S. P.; Steppan, C. M.; Stewart, A. E.; Tuttle, J. B.; Updyke, L.; Verhoest, P. R.; Wei, L.; Yang, Q.; Zhu, Y. An Oral SARS-CoV-2 M^{pro} Inhibitor Clinical Candidate for the Treatment of COVID-19. *Science* **2021**, *374*, 1586−1593.

(8) Ahmad, B.; Batool, M.; ul Ain, Q.; Kim, M. S.; Choi, S. Exploring the Binding Mechanism of PF-07321332 SARS-CoV-2 Protease Inhibitor through Molecular Dynamics and Binding Free Energy Simulations. *Int. J. Mol. Sci.* **2021**, *22*, 9124.

(9) Halford, B. The Path to Paxlovid. *ACS Cent. Sci.* **2022**, *8*, 405−407.

(10) Wild, C.; Greenwell, T.; Matthews, T. A Synthetic Peptide from HIV-1 Gp41 Is a Potent Inhibitor of Virus-Mediated Cell—Cell Fusion. *AIDS Res. Hum. Retroviruses* **1993**, *9*, 1051−1053.

(11) Miller, E. H.; Harrison, J. S.; Radoshitzky, S. R.; Higgins, C. D.; Chi, X.; Dong, L.; Kuhn, J. H.; Bavari, S.; Lai, J. R.; Chandran, K. Inhibition of Ebola Virus Entry by a C-Peptide Targeted to Endosomes. *J. Biol. Chem.* **2011**, *286*, 15854−15861.

(12) Jackson, C. B.; Farzan, M.; Chen, B.; Choe, H. Mechanisms of SARS-CoV-2 Entry into Cells. *Nat. Rev. Mol. Cell Biol.* **2022**, *23*, 3−20.

(13) Wrapp, D.; Wang, N.; Corbett, K. S.; Goldsmith, J. A.; Hsieh, C.-L.; Abiona, O.; Graham, B. S.; McLellan, J. S. Cryo-EM Structure of the 2019-NCoV Spike in the Prefusion Conformation. *Science* **2020**, *367*, 1260−1263.

(14) Cao, W.; Dong, C.; Kim, S.; Hou, D.; Tai, W.; Du, L.; Im, W.; Zhang, X. F. Biomechanical Characterization of SARS-CoV-2 Spike RBD and Human ACE2 Protein-Protein Interaction. *Biophys. J.* **2021**, *120*, 1011−1019.
(15) Jaimes, J. A.; Millet, J. K.; Whittaker, G. R. Proteolytic Cleavage of the SARS-CoV-2 Spike Protein and the Role of the Novel S1/S2 Site. *iScience* **2020**, *23*, No. 101212.
(16) Xia, S.; Zhu, Y.; Liu, M.; Lan, Q.; Xu, W.; Wu, Y.; Ying, T.; Liu, S.; Shi, Z.; Jiang, S.; Lu, L. Fusion Mechanism of 2019-NCoV and Fusion Inhibitors Targeting HR1 Domain in Spike Protein. *Cell Mol. Immunol.* **2020**, *17*, 765−767.
(17) Villa, A.; Brunialti, E.; Dellavedova, J.; Meda, C.; Rebecchi, M.; Conti, M.; Donnici, L.; De Francesco, R.; Reggiani, A.; Lionetti, V.; Ciana, P. DNA Aptamers Masking Angiotensin Converting Enzyme 2 as an Innovative Way to Treat SARS-CoV-2 Pandemic. *Pharmacol. Res.* **2022**, *175*, No. 105982.
(18) Yan, R.; Zhang, Y.; Li, Y.; Xia, L.; Guo, Y.; Zhou, Q. Structural Basis for the Recognition of SARS-CoV-2 by Full-Length Human ACE2. *Science* **2020**, *367*, 1444−1448.
(19) Benton, D. J.; Wrobel, A. G.; Xu, P.; Roustan, C.; Martin, S. R.; Rosenthal, P. B.; Skehel, J. J.; Gamblin, S. J. Receptor Binding and Priming of the Spike Protein of SARS-CoV-2 for Membrane Fusion. *Nature* **2020**, *588*, 327−330.
(20) Sadremomtaz, A.; Al-Dahmani, Z. M.; Ruiz-Moreno, A. J.; Monti, A.; Wang, C.; Azad, T.; Bell, J. C.; Doti, N.; Velasco-Velázquez, M. A.; de Jong, D.; de Jonge, J.; Smit, J.; Dömling, A.; van Goor, H.; Groves, M. R. Synthetic Peptides That Antagonize the Angiotensin-Converting Enzyme-2 (ACE-2) Interaction with SARS-CoV-2 Receptor Binding Spike Protein. *J. Med. Chem.* **2022**, *65*, 2836−2847.
(21) Larue, R. C.; Xing, E.; Kenney, A. D.; Zhang, Y.; Tuazon, J. A.; Li, J.; Yount, J. S.; Li, P.-K.; Sharma, A. Rationally Designed ACE2-Derived Peptides Inhibit SARS-CoV-2. *Bioconjugate Chem.* **2021**, *32*, 215−223.
(22) Han, Y.; Král, P. Computational Design of ACE2-Based Peptide Inhibitors of SARS-CoV-2. *ACS Nano* **2020**, *14*, 5143−5147.
(23) Zhang, G.; Pomplun, S.; Loftis, A. R.; Tan, X.; Loas, A.; Pentelute, B. L. Investigation of ACE2 N-Terminal Fragments Binding to SARS-CoV-2 Spike RBD. *Bioengineering* **2020**, DOI: 10.1101/2020.03.19.999318. preprint
(24) Nick Pace, C.; Martin, S. J. A Helix Propensity Scale Based on Experimental Studies of Peptides and Proteins. *Biophys. J.* **1998**, *75*, 422−427.
(25) Karoyan, P.; Vieillard, V.; Gómez-Morales, L.; Odile, E.; Guihot, A.; Luyt, C.-E.; Denis, A.; Grondin, P.; Lequin, O. Human ACE2 Peptide-Mimics Block SARS-CoV-2 Pulmonary Cells Infection. *Commun. Biol.* **2021**, *4*, 197.
(26) Odolczyk, N.; Marzec, E.; Winiewska-Szajewska, M.; Poznański, J.; Zielenkiewicz, P. Native Structure-Based Peptides as Potential Protein−Protein Interaction Inhibitors of SARS-CoV-2 Spike Protein and Human ACE2 Receptor. *Molecules* **2021**, *26*, 2157.
(27) Hack, V.; Reuter, C.; Opitz, R.; Schmieder, P.; Beyermann, M.; Neudörfl, J.-M.; Kühne, R.; Schmalz, H.-G. Efficient α-Helix Induction in a Linear Peptide Chain by *N*-Capping with a Bridged-Tricyclic Diproline Analogue. *Angew. Chem., Int. Ed.* **2013**, *52*, 9539−9543.
(28) Engelhardt, P. M.; Florez-Rueda, S.; Drexelius, M.; Neudörfl, J.; Lauster, D.; Hackenberger, C. P. R.; Kühne, R.; Neundorf, I.; Schmalz, H. Synthetic A-Helical Peptides as Potential Inhibitors of the ACE2 SARS-CoV-2 Interaction. *ChemBioChem* **2022**, *23*, No. e202200372.
(29) Zhang, Y.; Guo, J.; Cheng, J.; Zhang, Z.; Kang, F.; Wu, X.; Chu, Q. High-Throughput Screening of Stapled Helical Peptides in Drug Discovery. *J. Med. Chem.* **2023**, *66*, 95−106.
(30) de Araujo, A. D.; Hoang, H. N.; Kok, W. M.; Diness, F.; Gupta, P.; Hill, T. A.; Driver, R. W.; Price, D. A.; Liras, S.; Fairlie, D. P. Comparative α-Helicity of Cyclic Pentapeptides in Water. *Angew. Chem., Int. Ed.* **2014**, *53*, 6965−6969.
(31) Maas, M. N.; Hintzen, J. C. J.; Löffler, P. M. G.; Mecinović, J. Targeting SARS-CoV-2 Spike Protein by Stapled HACE2 Peptides. *Chem. Commun.* **2021**, *57*, 3283−3286.
(32) Monfette, S.; Fogg, D. E. Equilibrium Ring-Closing Metathesis. *Chem. Rev.* **2009**, *109*, 3783−3816.
(33) Curreli, F.; Victor, S. M. B.; Ahmed, S.; Drelich, A.; Tong, X.; Tseng, C.-T. K.; Hillyer, C. D.; Debnath, A. K. Stapled Peptides Based on Human Angiotensin-Converting Enzyme 2 (ACE2) Potently Inhibit SARS-CoV-2 Infection *In Vitro*. *mBio* **2020**, *11*, e02451−e02420.
(34) Calugi, L.; Sautariello, G.; Lenci, E.; Mattei, M. L.; Coppa, C.; Cini, N.; Contini, A.; Trabocchi, A. Identification of a Short ACE2-Derived Stapled Peptide Targeting the SARS-CoV-2 Spike Protein. *Eur. J. Med. Chem.* **2023**, *249*, No. 115118.
(35) Han, S.; Zhao, G.; Wei, Z.; Chen, Y.; Zhao, J.; He, Y.; He, Y.-J.; Gao, J.; Chen, S.; Du, C.; Wang, T.; Sun, W.; Huang, Y.; Wang, C.; Wang, J. An Angiotensin-Converting Enzyme-2-Derived Heptapeptide GK-7 for SARS-CoV-2 Spike Blockade. *Peptides* **2021**, *145*, No. 170638.
(36) Shah, M.; Moon, S. U.; Kim, J. H.; Thao, T. T.; Goo, W. H. SARS-CoV-2 Pan-Variant Inhibitory Peptides Deter S1-ACE2 Interaction and Neutralize Delta and Omicron Pseudoviruses. *Comput. Struct. Biotechnol. J.* **2022**, *20*, 2042−2056.
(37) Cao, L.; Goreshnik, I.; Coventry, B.; Case, J. B.; Miller, L.; Kozodoy, L.; Chen, R. E.; Carter, L.; Walls, A. C.; Park, Y.-J.; Strauch, E.-M.; Stewart, L.; Diamond, M. S.; Veesler, D.; Baker, D. De Novo Design of Picomolar SARS-CoV-2 Miniprotein Inhibitors. *Science* **2020**, *370*, 426−431.
(38) Weißenborn, L.; Richel, E.; Hüseman, H.; Welzer, J.; Beck, S.; Schäfer, S.; Sticht, H.; Überla, K.; Eichler, J. Smaller, Stronger, More Stable: Peptide Variants of a SARS-CoV-2 Neutralizing Miniprotein. *Int. J. Mol. Sci.* **2022**, *23*, 6309.
(39) Panda, S. K.; Sen Gupta, P. S.; Biswal, S.; Ray, A. K.; Rana, M. K. ACE-2-Derived Biomimetic Peptides for the Inhibition of Spike Protein of SARS-CoV-2. *J. Proteome Res.* **2021**, *20*, 1296−1303.
(40) Basit, A.; Karim, A. M.; Asif, M.; Ali, T.; Lee, J. H.; Jeon, J. H.; Ur Rehman, S.; Lee, S. H. Designing Short Peptides to Block the Interaction of SARS-CoV-2 and Human ACE2 for COVID-19 Therapeutics. *Front. Pharmacol.* **2021**, *12*, No. 731828.
(41) Meldal, M.; Diness, F. Recent Fascinating Aspects of the CuAAC Click Reaction. *Trends Chem.* **2020**, *2*, 569−584.
(42) Meldal, M.; Tornøe, C. W. Cu-Catalyzed Azide−Alkyne Cycloaddition. *Chem. Rev.* **2008**, *108*, 2952−3015.
(43) Testa, C.; Papini, A. M.; Chorev, M.; Rovero, P. Copper-Catalyzed Azide-Alkyne Cycloaddition (CuAAC)-Mediated Macrocyclization of Peptides: Impact on Conformation and Biological Activity. *Curr. Top. Med. Chem.* **2018**, *18*, 591−610.
(44) Cantel, S.; Le Chevalier, I. A.; Scrima, M.; Levy, J. J.; DiMarchi, R. D.; Rovero, P.; Halperin, J. A.; D'Ursi, A. M.; Papini, A. M.; Chorev, M. Synthesis and Conformational Analysis of a Cyclic Peptide Obtained via *i* to *i* +4 Intramolecular Side-Chain to Side-Chain Azide−Alkyne 1, 3-Dipolar Cycloaddition. *J. Org. Chem.* **2008**, *73*, 5663−5674.
(45) Testa, C.; Scrima, M.; Grimaldi, M.; D'Ursi, A. M.; Dirain, M. L.; Lubin-Germain, N.; Singh, A.; Haskell-Luevano, C.; Chorev, M.; Rovero, P.; Papini, A. M. 1,4-Disubstituted-[1,2,3]Triazolyl-Containing Analogues of MT-II: Design, Synthesis, Conformational Analysis, and Biological Activity. *J. Med. Chem.* **2014**, *57*, 9424−9434.
(46) Jochim, A. L.; Miller, S. E.; Angelo, N. G.; Arora, P. S. Evaluation of Triazolamers as Active Site Inhibitors of HIV-1 Protease. *Bioorg. Med. Chem. Lett.* **2009**, *19*, 6023−6026.
(47) Kawamoto, S. A.; Coleska, A.; Ran, X.; Yi, H.; Yang, C.-Y.; Wang, S. Design of Triazole-Stapled BCL9 α-Helical Peptides to Target the β-Catenin/B-Cell CLL/Lymphoma 9 (BCL9) Protein−Protein Interaction. *J. Med. Chem.* **2012**, *55*, 1137−1146.
(48) Scrima, M.; Le Chevalier-Isaad, A.; Rovero, P.; Papini, A. M.; Chorev, M.; D'Ursi, A. M. Cu ^{I} -Catalyzed Azide−Alkyne Intramolecular *i* -to-(*i* +4) Side-Chain-to-Side-Chain Cyclization Promotes

https://doi.org/10.1021/acsomega.3c01436
ACS Omega 2023, 8, 22665−22672

the Formation of Helix-Like Secondary Structures. *Eur. J. Org. Chem.* **2010**, *2010*, 446−457.
(49) D'Ercole, A.; Sabatino, G.; Pacini, L.; Impresari, E.; Capecchi, I.; Papini, A. M.; Rovero, P. On-resin Microwave-assisted Copper-catalyzed Azide-alkyne Cycloaddition of H1-relaxin B Single Chain 'Stapled' Analogues. *Pept. Sci.* **2020**, *112*, No. e24159.
(50) Khandelwal, P.; Seth, S.; Hosur, R. V. CD and NMR Investigations on Trifluoroethanol-Induced Step-Wise Folding of Helical Segment from Scorpion Neurotoxin. *Eur. J. Biochem.* **1999**, *264*, 468−478.
(51) Campagna, S.; Vitoux, B.; Humbert, G.; Girardet, J. M.; Linden, G.; Haertle, T.; Gaillard, J. L. Conformational Studies of a Synthetic Peptide from the Putative Lipid-Binding Domain of Bovine Milk Component PP3. *J. Dairy Sci.* **1998**, *81*, 3139−3148.
(52) Quagliata, M.; Nuti, F.; Real-Fernandez, F.; Kirilova, K.; Santoro, F.; Carotenuto, A.; Papini, A. M.; Rovero, P. Glucopeptides Derived from Myelin-relevant Proteins and Hyperglucosylated Non-typeable *Haemophilus Influenzae* Bacterial Adhesin Cross-react with Multiple Sclerosis Specific Antibodies: A Step Forward in the Identification of Native Autoantigens in Multiple Sclerosis. *J. Pept. Sci.* **2023**, No. e3475.
(53) Micsonai, A.; Wien, F.; Bulyáki, É.; Kun, J.; Moussong, É.; Lee, Y.-H.; Goto, Y.; Réfrégiers, M.; Kardos, J. BeStSel: A Web Server for Accurate Protein Secondary Structure Prediction and Fold Recognition from the Circular Dichroism Spectra. *Nucleic Acids Res.* **2018**, *46*, W315−W322.

https://doi.org/10.1021/acsomega.3c01436
ACS Omega 2023, 8, 22665−22672